INTERNATIONAL JOURNAL OF REFRIGERATION 37 (2014) 92–98

Available online at www.sciencedirect.com

SciVerse ScienceDirect

journal homepage: www.elsevier.com/locate/ijrefrig

Experimental and numerical results of a high frequency rotating active magnetic refrigerator

J.A. Lozano [a,b,*], K. Engelbrecht [a], C.R.H. Bahl [a,**], K.K. Nielsen [a], J.R. Barbosa Jr. [b], A.T. Prata [b], N. Pryds [a]

[a] Department of Energy Conversion and Storage, Technical University of Denmark (DTU), Frederiksborgvej 399, DK-4000 Roskilde, Denmark

[b] POLO – Research Laboratories for Emerging Technologies in Cooling and Thermophysics, Department of Mechanical Engineering, Federal University of Santa Catarina (UFSC), Florianopolis, SC 88040-900, Brazil

ARTICLE INFO

Article history:
Received 22 April 2013
Received in revised form
18 July 2013
Accepted 3 September 2013
Available online 12 September 2013

Keywords:
Active magnetic regenerator
Magnetic refrigeration
Experiment
Numerical modelling
Parasitic losses analysis

ABSTRACT

Experimental results for a recently developed prototype magnetic refrigeration device at the Technical University of Denmark (DTU) were obtained and compared with numerical simulation results. A continuously rotating active magnetic regenerator (AMR) using 2.8 kg packed sphere regenerators of gadolinium (Gd) was employed. With operating frequencies up to 10 Hz and volumetric flow rates up to 600 L h^{-1}, the prototype has shown high performance and the results are consistent with predictions from numerical modelling. Magnetocaloric properties of the Gd spheres were obtained experimentally and implemented in a one-dimensional numerical AMR model that includes also the parasitic losses from the prototype. The temperature span for a thermal load of 200 W as a function of frequency was measured and modelled. Moreover, the temperature span dependence on the cooling capacity as a function of cycle frequency was determined. A detailed study of these parasitic losses was carried out experimentally and numerically.

© 2013 Elsevier Ltd and IIR. All rights reserved.

Réfrigérateur magnétique actif rotatif à haute fréquence: résultats expérimentaux et numériques

Mots clés : Régénérateur actif magnétique ; Froid magnétique ; Expérience ; Modélisation numérique ; Analyse des pertes parasitiques

1. Introduction

It has been suggested that high frequency AMR devices will allow for higher cooling power per mass of magnetocaloric material and temperature spans (Yu et al., 2010). Most of the developed magnetic refrigerators work with permanent magnets and gadolinium (Gd) as magnetocaloric regenerative bed. Okamura et al. (2007) obtained a maximum cooling

* *Corresponding author*. Tel.: +55 48 3721 7970; fax: +55 48 3234 5166.
** *Corresponding author*. Tel.: +45 46775491; fax: +45 46775858.
E-mail addresses: jaime@polo.ufsc.br, jaimealozano@gmail.com (J.A. Lozano), chrb@dtu.dk (C.R.H. Bahl).
0140-7007/$ – see front matter © 2013 Elsevier Ltd and IIR. All rights reserved.
http://dx.doi.org/10.1016/j.ijrefrig.2013.09.002

Nomenclature

Roman

c	specific heat, J kg^{-1} K^{-1}
H	magnetic field, A m^{-1}
M	magnetization, A m^{-1}
N	demagnetization factor, –
Δs_{mag}	magnetic entropy change, J kg^{-1} K^{-1}
T	temperature, K
ΔT_{ad}	adiabatic temperature change, K
$\dot{W}$	power, W

Greek

ε	porosity, –

Subscripts

0	zero field
appl	applied
free	without the valves
fric	friction loss
H	hot end
int	internal
sys	system with the valves

Abbreviations

AMR	Active magnetic regenerator
DTU	Technical University of Denmark
Gd	Gadolinium
MFT	Mean field theory

capacity of 140 W kg^{-1} at 0.5 Hz and a cooling capacity of 40 W kg^{-1} with a temperature span of 5 K with a magnetic field of 1.1 T. Tura and Rowe (2011) achieved a cooling capacity of 455 W kg^{-1} at 10 K span and no thermal load temperature span of 29 K with a magnetic field of 1.4 T and a maximum operating frequency of 4 Hz. Russek et al. (2010) demonstrated a maximum zero-span cooling capacity of 948 W kg^{-1} and a cooling capacity of 449 W kg^{-1} with a temperature span of 10 K at 4.7 Hz employing a magnetic field of 1.4 T.

Experimental results for the device presented in this work for cycle frequencies up to 10 Hz show that the performance begins to degrade at higher frequencies with the optimum operating frequency near 2 Hz. In order to understand the results, the system is studied using a 1D AMR model developed by Engelbrecht et al. (2007). During the modelling phase of this work, focus was put on using accurate magnetocaloric properties as an input for the model, understanding frequency-dependent parasitic losses and understanding thermal parasitic losses. Magnetocaloric properties were measured on the commercial grade gadolinium taking into account the demagnetizing field in the measured sample. In the current experiments, frequency-dependent losses were studied while keeping all other operating conditions constant and the frequency was varied. The temperature span of the device decreases with increasing cooling power, allowing cooling curve experiments to be used to study thermal losses. The loss analysis is used to suggest design improvements.

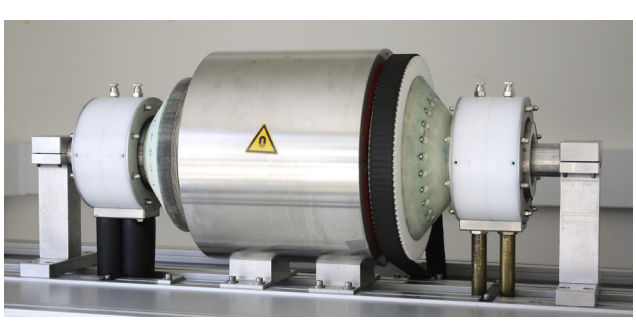

Fig. 1 – Rotating active magnetic refrigerator at DTU.

2. Experimental

Experiments on a rotating active magnetic refrigerator device at DTU (Fig. 1) working with a 4-pole static permanent magnet and 24 rotating regenerator beds were carried out at frequencies up to 10 Hz. The permanent magnet has a peak flux magnetic density of 1.24 T in the high field regions and it is close to 0 T in the low field regions (Bjørk et al., 2010). The regenerator beds consist of 99.99% pure commercial grade Gd spheres sieved to diameters between 0.25 and 0.8 mm and packed with a porosity of 0.36. The dimensions of the beds are 100 mm in the flow direction and a cross section of 12.5 mm width by 18.6 mm height. Each bed is connected to the valve by two separate channels dedicated to flow in and out of the bed, respectively. Thus, oscillating flow in the system is eliminated ensuring that losses due to mixing of fluid at different temperatures are avoided. The beds are rotated inside the magnet by an electrical motor with a variable rotation speed that is controlled by a frequency inverter. The volumetric fluid flow rate is manually controlled by a bypass valve at the outlet of a constant flow rate pump. At the cold end, the thermal load is simulated by an electric resistance heater, and the hot end temperature, T_H, is controlled by a heat exchanger in contact with a water chiller. More details on the design and operation of the device are presented in Bahl et al. (2011, 2014), Engelbrecht et al. (2012) and Lozano et al. (2013).

In this work, two different sets of experiments were carried out. First, the temperature span as a function of the frequency with a constant thermal load of 200 W was investigated. Then, the temperature span as a function of the cooling capacity at different frequencies was examined. The experimental results were compared with numerical results from a one-dimensional numerical model described in Engelbrecht et al. (2007). The model was modified to simulate the conditions of this experimental device. A packed sphere bed correlation (Kaviany, 1995) was employed for heat transfer in the regenerator beds. For modelling purposes, the ambient temperature was assumed constant at 295 K, which is a good approximation of the room temperature during the experiments.

The Gd spheres were characterized by a LakeShore 7407 Vibrating Sample Magnetometer (VSM) and a custom-built Differential Scanning Calorimeter (DSC) described in

Jeppesen et al. (2008). The isothermal entropy change with magnetization, Δs_{mag}, was calculated from the magnetization data using a Maxwell relation. Zero-field specific heat, c_0, was measured in the DSC. Since specific heat, c, Δs_{mag}, and the adiabatic temperature change, ΔT_{ad}, are coupled through the entropy curves and the internal magnetic field, once two of these parameters are known then the third can be calculated (Engelbrecht and Bahl, 2010). Entropy curves as a function of temperature and internal magnetic field were implemented in the numerical model. The density of the Gd was assumed constant as 7901 kg m^{-3} and the thermal conductivity was taken as 11 W m^{-1} K^{-1}.

The demagnetization effects due to the geometry of the sample were not included in the calculations of Δs_{mag} since on the numerical model a demagnetization function was implemented to take into account this effect on the regenerator beds. The function is based on the demagnetization factor, temperature and magnetization characteristics of the magnetocaloric material on the regenerator bed. The average value of the internal magnetic field within the Gd spheres, H_{int}, is calculated from the applied magnetic field in the absence of the bed, H_{appl}, and the overall average demagnetizing factor calculated from the shape of the bed, N, as given in Eq. (1) (Bleaney and Hull, 1941):

$$H_{int} = H_{appl} - M\left[\frac{1}{3} + (1-\varepsilon)\left(N - \frac{1}{3}\right)\right] \quad (1)$$

where M is the magnetization and ε is the porosity (equal to 0.36). For the actual regenerator beds, N is calculated to be 0.383 through the equation proposed by Aharoni (1998) using the dimensions of the beds and considering that the magnetic field is applied parallel to the height.

The heat transfer fluid used for the experiments is a mixture of 20% automotive antifreeze (ethylene-glycol) and 80% deionised water by volume. The antifreeze includes corrosion inhibitors that protect the Gd spheres while reducing the freezing temperature of the fluid. The thermodynamic properties of this mixture were obtained from Melinder (1997) and implemented in the numerical model as polynomial fits.

The thermal losses in the AMR correspond to losses from the cold end of the AMR to ambient (the room), from both the regenerators and from the external piping and equipments. Of the external components the connecting pipes, the heater and the flowhead were insulated during the experiments in this work.

3. Results and discussion

Magnetocaloric properties of the commercial Gd spheres employed in the regenerator beds are presented in Fig. 2. A peak of Δs_{mag} of 3.2 J kg^{-1} K^{-1} at a magnetic field change of 1 T was measured at a temperature of 288 K. Also, the peak of ΔT_{ad} of 3.1 K at 1 T and 289.6 K was calculated from entropy and specific heat data. These properties are lower than for those of pure Gd (Dan'kov et al., 1998) or from the ones calculated with the mean field theory (MFT) (Petersen et al., 2008). The difference is probably due to impurities and possibly corrosion

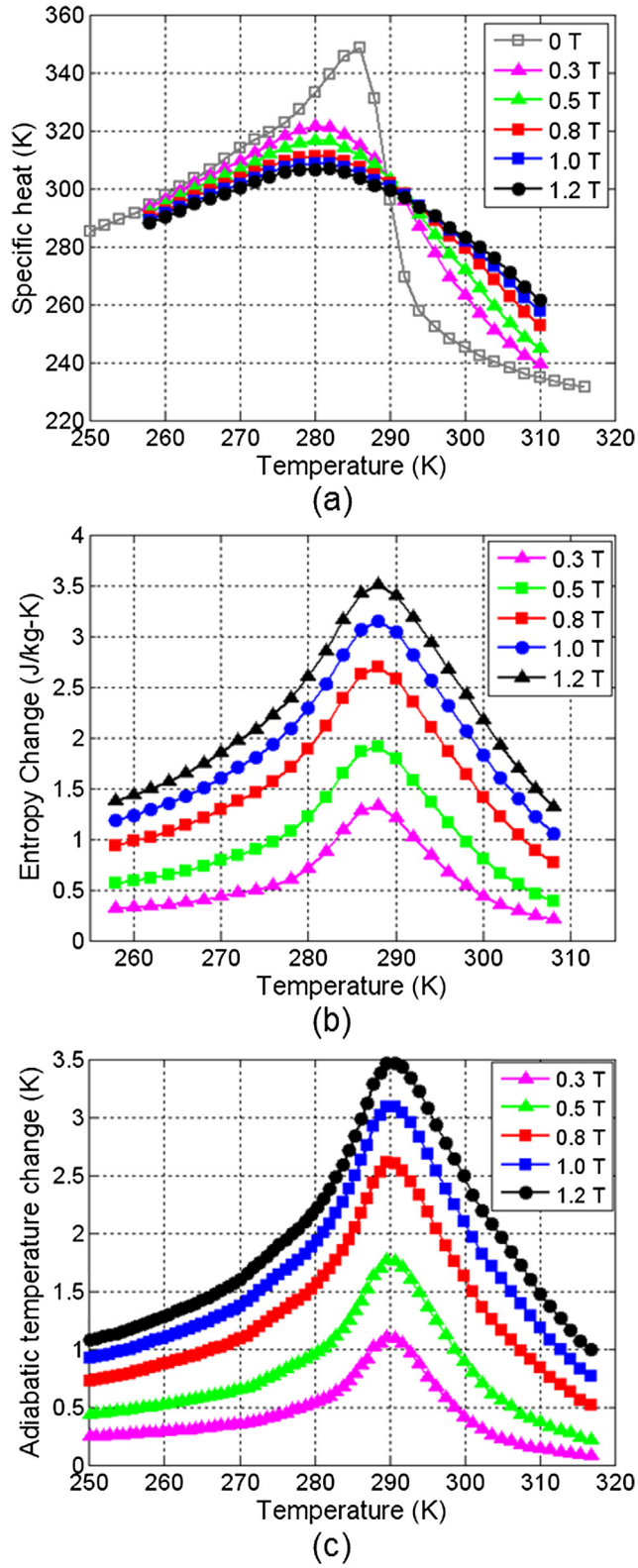

Fig. 2 – Properties of commercial Gd spheres used in the regenerator beds (a) Specific heat (zero-field is measured, the other curves are derived from Δs_{mag} from magnetization data and the zero-field specific heat) (b) Δs_{mag} integrated from the specific heat, and (c) ΔT_{ad} as a function of temperature and magnetic field (derived from the specific heat and Δs_{mag} data).

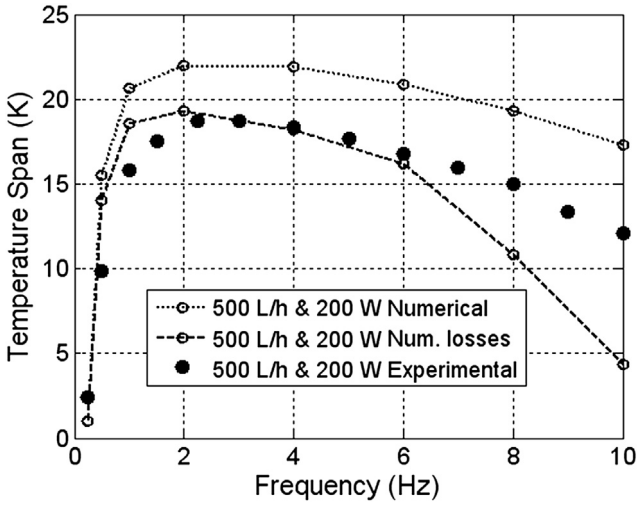

Fig. 3 – Experimental and numerical results for the temperature span as a function of frequency with a cooling capacity of 200 W and T_H = 298 K.

on Gd spheres (Dan'kov et al., 1998). Also, the measured Curie temperature seems to be lower than that published for pure Gd (Pecharsky et al., 2001). Therefore, numerical results obtained with these properties are expected to have lower performance and a lower peak temperature than results obtained with pure Gd properties would have.

The temperature span dependence on the operation frequency for a cooling capacity of 200 W is shown in Fig. 3. This experiment was performed with a constant volumetric flow rate of 500 L h^{-1}, which was measured at the cold end. The chiller temperature was also kept constant in order to maintain T_H at approximately 298 K. A peak on the temperature span of 18.9 K was attained for an operation frequency of 2.25 Hz. At lower frequencies there is a large influence of the longitudinal thermal conduction (Nielsen et al., 2011) and the regenerator utilization becomes too high. However, it can be seen that at lower frequencies, normally those used in most AMR devices, the temperature span increases with increasing frequency, as observed experimentally in Russek et al. (2010), until a certain optimum frequency from which the irreversible losses become significant and the heat transfer is affected, so the regenerator is not able to maintain a high temperature span. This trend of the temperature span obtained experimentally is in agreement with published numerical results for other conditions (Tusek et al., 2011).

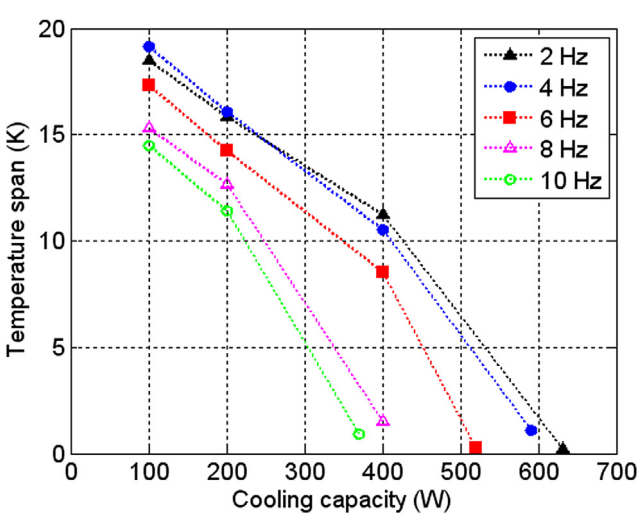

Fig. 4 – Experimental results of the temperature span as a function of the cooling capacity at different frequencies and T_H = 296 K.

A detailed study of the behaviour of the device at high frequencies was carried out by experiments of the temperature span as a function of the cooling capacity at different frequencies and the results are shown in Fig. 4. In these experiments the volumetric flow rate was held constant at 500 L h^{-1}. Due to a lower Curie temperature of the Gd, an improvement of the performance at higher cooling capacities was expected to be obtained at lower T_H. Consequently, for this set of experiments the T_H was set at approximately 296 K. A detailed study of the hot reservoir temperature dependence on this refrigerator is presented in Lozano et al. (2013).

These results are in agreement with those in Fig. 3, where the best performance is achieved at a frequency of approximately 2 Hz. This is due mainly to heat generation in the valves at higher frequencies caused by friction between the seals and the flowhead, as well as, other thermal parasitic losses with the ambient. Therefore, a thermal loss analysis was carried out to evaluate their influence on the temperature difference and of the operating conditions of the device at high frequencies. Absolute parasitic thermal resistances based on geometrical shape, estimated free convection losses and material properties of the regenerator housing and cold end components to the ambient were calculated to be 0.23, 5.75 and 13.88 K W^{-1} for the regenerator, flowhead and connecting tubes, respectively. Due to the complexity of the geometry of the flowhead, a 2D numerical simulation was carried out in COMSOL to determine its overall thermal resistance and by including a 2 mm thick foam insulation. The thermal resistances of the regenerator and the connecting tubes were calculated supposing that the heat transport phenomena occur by conduction through the walls and internal and external convection due to the temperature difference between the fluid and the ambient. A more in-depth study of the parasitic losses is outside the scope of this work. A more detailed thermal loss analysis of this refrigerator can be found in Lozano et al. (2013). These thermal losses are considerable at higher temperature spans, when the cold end is working in temperatures lower than the ambient temperature. These losses are post calculated and then deducted from the predicted cooling power of the device. The influences of these losses on the regenerator cycle are therefore not accounted for.

Regarding the losses by friction in the valve, some measurements were carried out to calculate the power that the motor consumes due to this friction, $\dot{W}_{fric}$. The friction loss is simply the difference in power required to rotate the machine with and without the seals (Eq. (2))

$$\dot{W}_{fric} = \dot{W}_{sys} - \dot{W}_{free} \tag{2}$$

where $\dot{W}_{sys}$ correspond to the power used to operate the system with the valves and $\dot{W}_{free}$ is the power of operation without the valves. Since these powers are a function of

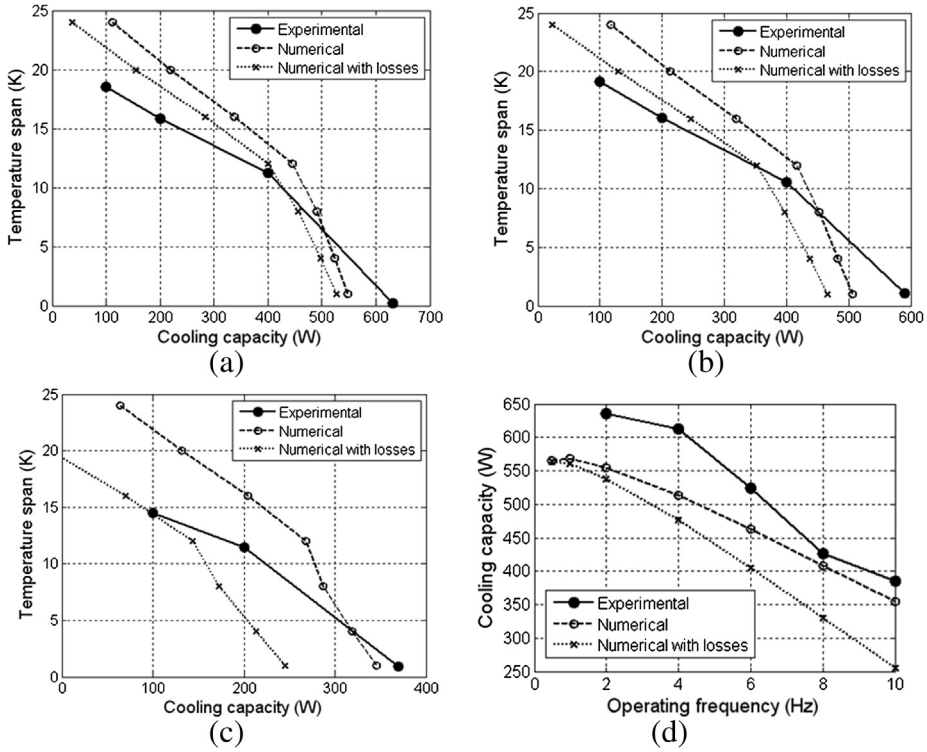

Fig. 5 – Comparison of experimental and numerical results at (a) 2 Hz, (b) 4 Hz and (c) 10 Hz and (d) Maximum cooling capacity at no-span.

frequency and temperature, experiments were performed at room-temperature with no flow and no temperature span, but varying frequencies. It was found that $\dot{W}_{fric}$ increases almost linearly with frequency and an average of $\dot{W}_{fr}$ ~40 W per Hz was calculated. This value corresponds to the power consumed due to the valve at both the hot and cold ends of the device and it is assumed that the heat generated in both is equal. However, heat leaks at the hot end are neglected because they are not a major performance parameter. Taking into account that at temperatures below room-temperature there is a contraction of the nylon in the flowhead and that only part of the heat generated is dissipated into the cold stream of fluid, the equivalent heat dissipated by the valve to the fluid is assumed to be approximately half of the heat generated by valve which is about 10 W per Hz. Therefore, at 2 Hz the thermal loss due to the friction at the valve is about 20 W, while at 10 Hz the loss is approximately 100 W.

As a result, an overall heat loss value was calculated for each experiment as the sum of the thermal parasitic losses on the components and the heat generated by friction on the valve. This heat loss was subtracted from the cooling capacity found by numerical simulation and the results are plotted in Fig. 3 for the temperature span as a function of operating frequency. The results for temperature span as a function of cooling capacity are compared to the experimental results at 2, 4 and 10 Hz as shown in Fig. 5(a–c), respectively. The maximum cooling capacity at no-span as a function of the operating frequency is presented in Fig. 5(d).

As can be seen in Fig. 3, the agreement between model and experiment is acceptable when losses are deducted from the model results until the cycle frequency increases above 6 Hz. This is most likely due to an inaccurate model of the valve friction that was implemented. Valve friction is assumed to be linear with increasing rotation speed, but the actual friction could be a complex function of fluid dynamics in the rotary seal and the absolute fluid pressure and temperature. The experimental data suggest that the valve friction is over predicted at high cycle frequency. In Fig. 5, the model is in good agreement with experiment except at the lowest temperature spans, which correspond to the highest cooling powers. In each maximum cooling case, the temperature span is less than 2 K and the material is operating near its Curie temperature. Because the average magnetocaloric properties in the regenerator are highly sensitive to temperature near the Curie temperature, the discrepancy between model and experiment could be caused by either an error in the measured Curie temperature of material or by uncertainty in the absolute temperature measured in the thermocouples.

From the numerical results can be inferred that the irreversible thermal losses increase with the frequency. At low cooling capacities, or high temperature spans, the model over predicts the measured results. This may be related to the fact that the numerical model does not include some other thermal losses, such as those at the boundaries of the regenerator bed (in this model they are considered adiabatic), where a heat leak is present with the housing and ambient which becomes higher when the cold end is below room-temperature. Nielsen et al. (2009) affirmed that this effect may have a considerable impact on the AMR performance. Other types of thermal losses not taken into account in this work are the magnetic losses

in Gd beds due to the parasitic currents produced by the magnetization and demagnetization of the magnetic material at relative higher frequencies. At the cold-end there are other heat sinks in the device such as the filter, valve and mass flowmeter which were not included in the calculations. There are other uncertainties in the numerical model such as the particle size distribution which was employed. It was found that the measured theoretical pressure drop based on the Ergun equation (Ergun, 1952) results for a monodisperse matrix regenerator of 0.6 mm diameter spheres is in good agreement with the average experimental pressure drop of the actual regenerator beds employed in this work.

From this thermal analysis some design improvements for further AMR devices operating at higher frequencies are proposed. First, some effort should be taken into account for the design of the valves or system that allows oscillatory flow in the regenerator beds and valve friction must be avoided as much as possible. This parasitic loss could be diminished by decreasing the contact area between the sealing surfaces or by employing a single rotary valve only at the hot end. Good thermal insulation should be used in the cold end and along the regenerator beds to avoid heat leaks while working below room-temperature. The cold end should be simplified and compact in order to decrease the surface area for heat leakage with the ambient.

It was proven through modelling in this work, as Tusek et al. (2011) proposed, that smaller sphere diameters lead to higher temperature spans and cooling capacities at high frequencies, due to an increase in heat transfer area and heat transfer coefficient. However, decreasing particle size represents a pronounced increase in viscous losses and pressure drop along the bed increasing pumping power and thus decreasing the performance of the device.

The performance of the device could also be improved by increasing the volumetric flow rate when operating at higher frequencies. Thus, a good hydraulic system design, which allows higher flows with tolerable pressure drop, is recommended for further magnetic refrigerator designs.

4. Conclusion

Experimental and numerical results for a high frequency rotating active magnetic refrigerator were obtained. Temperature span was measured at frequencies up to 10 Hz. An experimental peak on the temperature span of 18.9 K with 200 W cooling capacity was attained at 2.25 Hz. The observed trend of the experimental temperature span agrees well with that published in the literature for both experimental and numerical data. A thermal analysis was performed to evaluate the thermal losses which have higher impacts on the performance of the device, such as the heat generated due to friction at the valve and the thermal leaks to the ambient. The former is directly proportional to the frequency while the latter depends on the temperature difference from the ambient. These losses were taken into account in the 1D AMR model, and the results agree well the experimental data for temperature span as a function of frequency and cooling capacity. A more efficient hydraulic system design, including the valve design, is proposed to improve the performance of the device at high frequencies, better insulation at the cold end and smaller sphere diameters are proposed as improvements for future AMR devices working at high frequencies.

Acknowledgements

The authors would like to acknowledge the support of the Programme Commission on Energy and Environment (EnMi) (Contract No. 2104-06-0032) which is part of the Danish Council for Strategic Research. The authors thank Jørgen Geyti for technical assistance. J.A. Lozano, J.R. Barbosa and A.T. Prata thank the financial support from CNPq (Brazil) through Grant No. 18573581/2008-8 (National Institute of Science and Technology in Cooling and Thermophysics). K.K. Nielsen wishes to thank The Danish Council for Independent Research|Technology and Production Sciences (Contract no. 10-092791) for financial support.

REFERENCES

Aharoni, A., 1998. Demagnetizing factors for rectangular ferromagnetic prisms. J. Appl. Phys. 83 (6), 3432–3434.

Bahl, C.R.H., Engelbrecht, K., Bjørk, R., Eriksen, D., Smith, A., Nielsen, K.K., Pryds, N., 2011. Design concepts for a continuously rotating active magnetic regenerator. Int. J. Refrigeration 34 (8), 1792–1796.

Bahl, C.R.H., Engelbrecht, K., Eriksen, D., Lozano, J.A., Bjørk, R., Geyti, J., Nielsen, K.K., Smith, A., Pryds, N., 2014. Development and experimental results from a 1 kW near continuous prototype AMR. Int. J. Refrigeration 37, 78–83.

Bleaney, B., Hull, R.A., 1941. The effective susceptibility of a paramagnetic powder. Proc. R. Soc. 178 (972), 86–92.

Bjørk, R., Bahl, C.R.H., Smith, A., Christensen, D.V., Pryds, N., 2010. An optimized magnet for magnetic refrigeration. J. Magnetism Magn. Mater. 322, 3324–3328.

Dan'kov, S.Y., Tishin, A.M., Pecharsky, V.K., Gschneidner Jr., K.A., 1998. Magnetic phase transitions and the magnetothermal properties of gadolinium. Phys. Rev. B 57 (6), 3478–3490.

Engelbrecht, K., Nellis, G., Klein, S., Zimm, C., 2007. Recent developments in room temperature active magnetic regenerative refrigeration. HVAC&R Res. 13 (4), 525–542.

Engelbrecht, K., Bahl, C.R.H., 2010. Evaluating the effect of magnetocaloric properties on magnetic refrigeration performance. J. Appl. Phys. 108, 123918.

Engelbrecht, K., Eriksen, D., Bahl, C.R.H., Bjørk, R., Geyti, J., Lozano, J.A., Nielsen, K.K., Saxild, F., Smith, A., Pryds, N., 2012. Experimental results for a novel rotary active magnetic regenerator. Int. J. Refrigeration 35 (6), 1498–1505.

Ergun, S., 1952. Fluid flow through packed columns. Chem. Eng. Prog. 48 (2), 89–94.

Jeppesen, S., Linderoth, S., Pryds, N., Theil Kuhn, L., Buch Jensen, J., 2008. Indirect measurement of the magnetocaloric effect using a novel differential scanning calorimeter with magnetic field. Rev. Sci. Instrum. 79, 083901.

Kaviany, M., 1995. Principles of Heat Transfer in Porous Media. Springer, New York.

Lozano, J.A., Engelbrecht, K., Bahl, C.R.H., Nielsen, K.K., Eriksen, D., Olsen, U.L., Barbosa Jr., J.R., Smith, A., Prata, A.T., Pryds, N., 2013. Performance analysis of a rotary active magnetic refrigerator. Appl. Energy 111, 669–680.

Melinder, A., 1997. Thermophysical Properties of Liquid Secondary Refrigerants. International Institute of Refrigeration, Paris.

Nielsen, K.K., Bahl, C.R.H., Bjørk, R., Pryds, N., Smith, A., Hattel, J., 2009. Detailed numerical modeling of a linear parallel-plate active magnetic regenerator. Int. J. Refrigeration 32, 1478–1486.

Nielsen, K.K., Tusek, J., Engelbrecht, K., Schopfer, S., Kitanovski, A., Bahl, C.R.H., Smith, A., Pryds, N., Poredos, A., 2011. Review on numerical modeling of active magnetic regenerators for room temperature applications. Int. J. Refrigeration 34 (3), 603–616.

Okamura, T., Rachi, R., Hirano, N., Nagaya, S., 2007. Improvement of 100 W class room temperature magnetic refrigerator. In: Proceedings of the 2nd International Conference of Magnetic Refrigeration at Room Temperature. Portoroz, Slovenia, pp. 377–382.

Pecharsky, V.K., Gschneidner, K.A., Pecharsky, A.O., Tishin, A.M., 2001. Thermodynamics of the magnetocaloric effect. Phys. Rev. B 64 (14), 144406/1–14440613.

Petersen, T.F., Pryds, N., Smith, A., Hattel, J., Schmidt, H., Knudsen, H.J.H., 2008. Two-dimensional mathematical model of a reciprocating room-temperature active magnetic regenerator. Int. J. Refrigeration 31, 432–443.

Tura, A., Rowe, A., 2011. Permanent magnet magnetic refrigerator design and experimental characterization. Int. J. Refrigeration 34, 628–e639.

Russek, S., Auringer, J., Boeder, A., Chell, J., Jacobs, S., Zimm, C., 2010. The performance of a rotary magnet magnetic refrigerator with layered beds. In: Proc. 4th Int. Conference on Magnetic Refrigeration at Room Temperature, Baotou, Inner Mongolia, China, pp. 339–349.

Tusek, J., Kitanovski, A., Prebil, I., Poredos, A., 2011. Dynamic operation of an active magnetic regenerator (AMR): numerical optimization of a packed-bed AMR. Int. J. Refrigeration 34, 1507–1517.

Yu, B., Liu, M., Egolf, P.W., Kitanovski, A., 2010. A review of magnetic refrigerator and heat pump prototypes built before the year 2010. Int. J. Refrigeration 33, 1029–1060.